6th International Conference on Advances in Experimental Structural Engineering
11th International Workshop on Advanced Smart Materials and Smart Structures Technology
August 1-2, 2015, University of Illinois, Urbana-Champaign, United States

A GENERALIZED CONSTITUTIVE MODEL FOR ELASTOMERIC BEARINGS

Wei Wei[1], Yong Yuan[2,*]

1 *Doctoral student, Dept. of Civil Engineering & Mechanics, Huazhong University of Science &Technology, China*
E-mail:weiwei198907@163.com

2 *Associate professor, Dept. of Civil Engineering & Mechanics, Huazhong University of Science &Technology, China*
E-mail: yuanyong@hust.edu.cn

ABSTRACT

Elastomeric bearings have been a mature technique to mitigate the damage of earthquakes on structures. However, too many constitutive models for elastomeric bearings lead to a particularly complex analysis and design of the isolated structure. This paper developed a general rate-dependent constitutive model which allows accurate description of force-displacement relationship for natural rubber bearing (NRB), high damping rubber bearing (HDRB) and super high damping rubber bearing (SHDRB). The proposed constitutive model is composed of two hyperelastic springs and a nonlinear dashpot element, which following the finite deformation viscoelasticity laws based on classical Zener model. Fletcher-Gent effect, high horizontal stiffness at small strains causing by the carbon fillers in the elastomeric bearings, is modeled accurately through the additional stiffness parameter α in the novel strain energy function. On the basis of conducted laboratory tests including multi-step relaxation and monotonic shear tests, a parameter identification scheme is implemented. Finally, by comparing the numerical simulation and test results, it is found that the proposed constitutive model is capable of well predicting the stress-strain relationship of elastomeric bearings at different strain rates.

KEYWORDS: *elastomeric bearing, constitutive law, rate-dependency*

1. INTRODUCTION

Elastomeric bearings have been widely used as seismic isolators to protect buildings and bridges from earthquake damages. Among various types of elastomeric bearings, natural rubber bearing (NRB) and lead rubber bearing (LRB) have been well known and the application of them in civil structures has increased substantially during the last decades. The NRB uses alternate layers of natural rubbers and steel plates, LRB inserts one or more lead plugs into the NRB to enhance hysteretic damping and initial stiffness of the bearing. However, because lead material is a toxic substance for environment, the application of LRB will gradually diminish in the future. In recent years, two evolving types of elastomeric bearings were invented, named as high damping rubber bearing (HDRB) and super high damping rubber bearing (SHDRB). The rubber material of HDRB and SHDRB possesses high damping due to the add of chemical fillers including carbon black, plasticizer and oil during the vulcanization process.

* Correspondent author at: Department of Civil Engineering & Mechanics, Huazhong University of Science &Technology, Wuhan, China.

Since the acceptance of the performance-based design philosophy, some design specifications [1] recommend the use of nonlinear time history analysis for the seismic response assessment of isolated bridges. In those specifications, the hysteretic behavior of NRB is approximated by equivalent linear (EL) method, and that of HDRB and SHDRB are represented by bilinear model. However, the chemical fillers in rubber make the hysteretic behavior of the elastomeric bearings, in particular the HDRB and SHDRB, considerably complicated. Therefore, both equivalent linear and bilinear models cannot reproduce the nonlinear elasto-plastic characteristic especially the rate-dependent property as found by many researchers [2-3].

In this paper, a general rate-dependent constitutive law for three types of elastomeric bearings (i.e. HRB, HDRB, and SHDRB) under the horizontal shear deformation is established. In formulating the mathematical expression of stress-strain function, an improved hyperelastic Zener model is developed and the total stress of rubber material is decomposed to rate-independent equilibrium stress and rate-dependent overstress to describe the fundamental viscoelastic behavior of the material. Moreover, a range of material tests including multi-step relaxation test and monotonic shear test are performed to identify the model parameters. Finally, the numerical and experimental results are compared to verify the accuracy of the proposed model.

2. STRAIN ENERGY FUNCTION

According to the phenomenological theory, rubber is assumed as a isotropic and incompressible material, the mechanical properties of a rubber can be characterized by its strain energy function W, which can be represented in terms of deformation tensor invariants (I_1, I_2, I_3),

$$W = W(I_1, I_2, I_3) \tag{2.1}$$

$$\begin{cases} I_1 = \lambda_1^2 + \lambda_2^2 + \lambda_3^2 \\ I_2 = \lambda_1^2\lambda_2^2 + \lambda_2^2\lambda_3^2 + \lambda_3^2\lambda_1^2 \\ I_3 = \lambda_1^2\lambda_2^2\lambda_3^2 \end{cases} \tag{2.2}$$

where $\lambda_i (i = 1,2,3)$ denote stretches in the three principal directions.
considering that rubber is incompressible, therefore, $I_3 = 1$, implying that W is expressed as a function of I_1 and I_2

There are many proposed strain energy function expressions in the literature, the most general strain energy function formulation is proposed by Rivlin [4]. However, most of the published researches are focusing on rubber-like materials [5], while the investigation of the behavior of elastomeric rubber material is found only in a few works. Therefore, development of an adequate strain energy function applicable to shear deformation is aroused by these reasons. In this study, a strain energy function of I_1 and I_2 with an additional stiffness correction factor α is proposed as follows:

$$W(I_1, I_2) = C_1(I_1 - 3) + \frac{2}{3}C_2(I_1 - 3)^{\frac{3}{2}} + \frac{1}{2}C_3(I_1 - 3)^2 + \frac{2}{5}C_4(I_1 - 3)^{\frac{5}{2}} + \frac{C_5}{\alpha + 1}(I_2 - 3)^{\alpha + 1} \tag{2.3}$$

where C_i $(i = 1-5)$ and α are the material model parameters.

3. CONSTITUTIVE EQUATION FOR RATE-DEPENDENT PROPERTY

To model the rate-dependent phenomenon of elastomeric bearings, a Zener model as illustrated in Figure 2.1 is considered. The hyperelastic spring A represents the rate-independent equilibrium stress, while the Maxwell element consisting of a hyperelastic spring B and a nonlinear dashpot C represent the rate-dependent overstress.

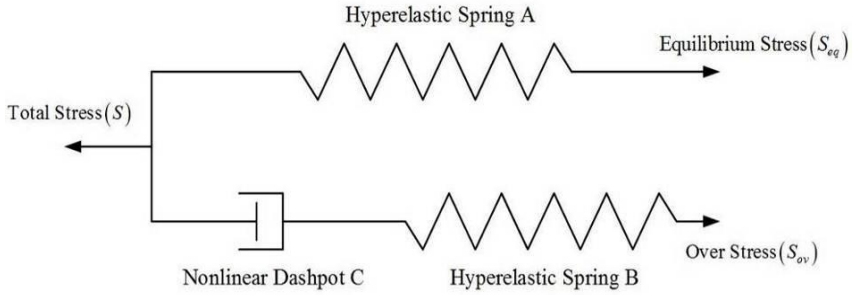

Figure 2.1 Schematic of modified hyperelastic Zener model

the Cauchy stress tensor $\mathbf{S}$ of rubber material is expressed as follows

$$\mathbf{S}_{ij} = 2\left[\mathbf{B}_{ij}\frac{\partial W}{\partial I_1} - \left(\mathbf{B}_{ij}\right)^{-1}\frac{\partial W}{\partial I_2}\right] - p\delta_{ij} \tag{3.1}$$

where δ_{ij} is the Kronecker symbol, and p is the hydrostatic pressure determined by the boundary condition.

For shear deformation, we have

$$\begin{cases} \lambda_2 = 1 \\ \lambda_3 = \lambda_1^{-1} \\ \gamma = \lambda_1 - \lambda_3 \end{cases} \tag{3.2}$$

the left Cauchy-Green deformation tensor $\mathbf{B}$ and $\mathbf{B}^{-1}$ can be calculated as follow

$$\mathbf{B}_{ij} = \begin{bmatrix} 1+\gamma^2 & \gamma & 0 \\ \gamma & \gamma & 0 \\ 0 & 0 & 1 \end{bmatrix} \tag{3.3}$$

$$(\mathbf{B}_{ij})^{-1} = \begin{bmatrix} 1 & -\gamma & 0 \\ -\gamma & 1+\gamma & 0 \\ 0 & 0 & 1 \end{bmatrix} \tag{3.4}$$

Substituting Eqs.(3.2)-(3.4) into Eq.(3.1), the shear stress component can be given by

$$\mathbf{S}_{12} = 2\gamma\left(\frac{\partial W}{\partial I_1} + \frac{\partial W}{\partial I_2}\right) \tag{3.5}$$

for equilibrium stress,

$$\tau_{eq} = 2\left(C_{1eq}\gamma_{eq} + C_{2eq}\gamma_{eq}^2 + C_{3eq}\gamma_{eq}^3 + C_{4eq}\gamma_{eq}^4 + C_{5eq}\gamma_{eq}^{2\alpha_{eq}+1}\right) \tag{3.6}$$

for overstress,

$$\tau_{ov} = 2\left(C_{1ov}\gamma_{ov} + C_{2ov}\gamma_{ov}^2 + C_{3ov}\gamma_{ov}^3 + C_{4ov}\gamma_{ov}^4 + C_{5ov}\gamma_{ov}^{2\alpha_{ov}+1}\right) \tag{3.7}$$

where C_{ieq}, C_{iov} (i=1~5) , α_{eq} and α_{ov} are the material model parameters determined by two responses: the first is the equilibrium response and another is the instantaneous response.

On the basis of Huber and Tsakmakis' s [6] finding, the rate of Left Cauchy-Green deformation tensor of the constitutive model is defined by

$$\dot{\mathbf{B}}_B = \mathbf{B}_B\mathbf{L}_A^T + \mathbf{L}_A\mathbf{B}_B - \frac{2}{\eta}\mathbf{B}_B\mathbf{S}_B{}^D \tag{3.8}$$

$$\mathbf{L} = \dot{\mathbf{F}}\cdot\mathbf{F}^{-1} \tag{3.9}$$

where η is a positive material viscosity parameter representing the dashpot. The $(\cdot)$ indicates material time derivative and the superscript D denotes the deviatoric component. $\mathbf{L}$ is the velocity gradient tensor defined by

$$\mathbf{L}=\dot{\mathbf{F}}\mathbf{F}^{-1} = \begin{bmatrix} 0 & \dot{\gamma} & 0 \\ 0 & 0 & 0 \\ 0 & 0 & 0 \end{bmatrix}\cdot\begin{bmatrix} 1 & -\gamma & 0 \\ 0 & 1 & 0 \\ 0 & 0 & 1 \end{bmatrix} = \begin{bmatrix} 0 & \dot{\gamma} & 0 \\ 0 & 0 & 0 \\ 0 & 0 & 0 \end{bmatrix} \tag{3.10}$$

combining Eqs.(3.8)-(3.10), the expression of rate of $\mathbf{B}_B$ is obtained.

4. MATERIAL TESTS AND PARAMETER IDENTIFICATION

4.1 Specimens and instruments

The test specimen consists of two rubber layers and three steel blocks, it has a net shear area of 25×20mm. Tests were conducted by using a computer-controlled servo hydraulic loading machine.

4.2 Multi-step relaxation test and monotonic shear test

It is impractical to obtain the equilibrium stress by means of loading tests with an infinitesimally slow loading rate. To address this problem, a multi–step relaxation (MSR) test was employed in the experimental scheme to obtain the equilibrium stress. In the present study, each rubber material specimen tested up to the specified strain levels and held constant with a time interval of 20 minutes, Figure 4.1presents the applied strain history utilized

in the test.

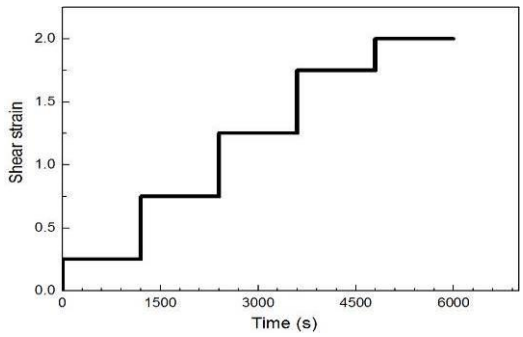

Figure 4.1 Applied strain histories in multi-step relaxation tests

Figure 4.2 shows the resultant stress histories obtained by MSR tests. It is clear seen that at the end of each relaxation interval of 20 minutes, each stress history converges to an almost constant value in both specimens. By connecting all the minimum stress values at each corresponding strain level, the equilibrium curve can be achieved.

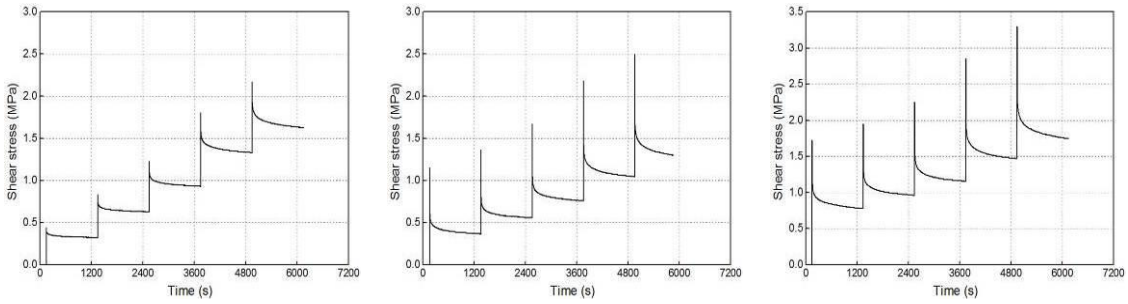

(a) NRB (b) HDRB (c) SHDRB

Figure 4.2 Stress time history obtained by multi-step relaxation tests

Theoretically, the instantaneous response can be ideally obtained when the rubber material is loaded at an infinitely fast rate. However, the maximum stroke velocity of the displacement controlled device inherently limits the loading rate of the specimen. In order to overcome this limitation, a series of monotonic shear tests were conducted shown in Figure 4.3. The tests were carried out at four different loading rates up to a maximum shear strain range of 200%. The four strain rates of 0.08, 0.8, 1.6 and 4.0 1/s were utilized in the tests correspond to frequencies of 0.01，0.1，0.2，0.5 Hz, respectively. The stress response obtained at 4.0 1/s is regarded as the neighborhood of the instantaneous response.

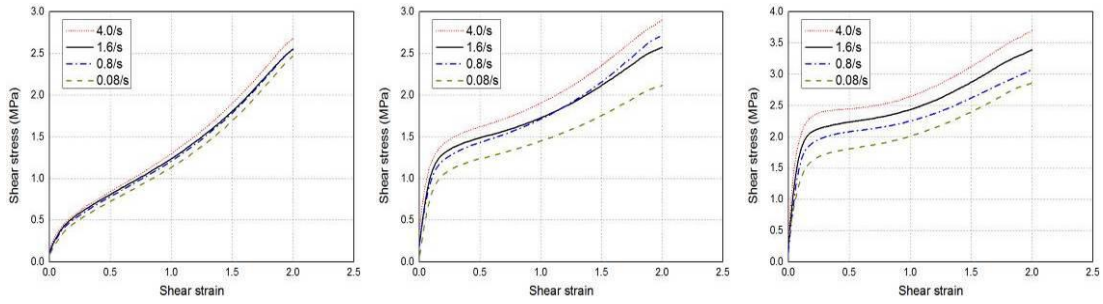

(a) NRB (b) HDRB (c) SHDRB

Figure 4.3 Shear stress-strain relationships obtained by monotonic shear tests

4.3 Material parameter identification

The parameters for equilibrium stress component can be determined by applying the least-square method to Eq.(3.6) with sets of the equilibrium stress τ_{eq} and corresponding shear strain γ_{eq} obtained by the multi-step relaxation test. The results of parameter identification are shown in Table 4.1.

Table 4.1 Material parameter for equilibrium stress

Specimen	C_{1eq} (MPa)	C_{2eq} (MPa)	C_{3eq} (MPa)	C_{4eq} (MPa)	C_{5eq} (MPa)
NRB	0.7642	-0.7091	0.3883	-0.0619	0
HDRB	1.0615	-1.5318	0.9779	-0.1994	0
SHDRB	2.0347	-3.0981	1.9878	-0.4239	0

The value of overstress τ_{ov} is obtained by subtracting the equilibrium stress τ_{eq} from the total stress obtained by the monotonic shear test using the case of 4.0 1/s strain rate case. Parameters C_{iov} (i=1~5) are determined by the least-square fitting method. The identified values of the overstress parameters are listed in Table 4.2.

Table 4.2 Material parameter for overstress

Specimen	C_{1ov} (MPa)	C_{2ov} (MPa)	C_{3ov} (MPa)	C_{4ov} (MPa)	C_{5ov} (MPa)	α_{ov}
NRB	0.3561	-0.4315	0.4666	-0.1399	0.0141	-0.35
HDRB	1.1306	-1.0488	0.7869	-0.2551	0.0264	-0.35
SHDRB	1.7699	-2.0761	1.7718	-0.7801	0.1346	-0.35

The viscosity coefficient η obtained from the tests results is found not to be constant, showing variation within the progress of deformation. In this study, the Gaussian function and a 3rd order polynomial function is proposed to describe the strain and strain rate dependence of η.

5. MODEL VALIDATION

To validate the proposed model, numerical simulations are compared with the experimental results. Figure

5.1-5.3 indicate the different strain-rate cases and it is found that all simulated values are well described the rate-dependent response at moderate and large strains along with high stiffness feature at small strains.

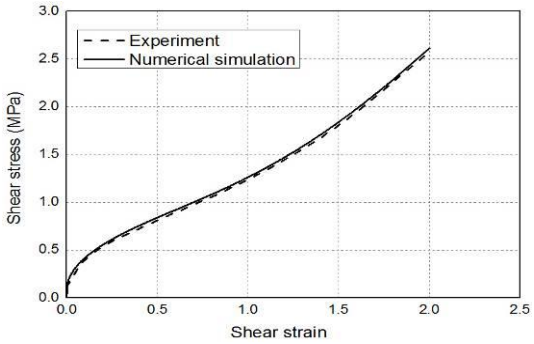

(a) Strain rate of 1.6 1/s

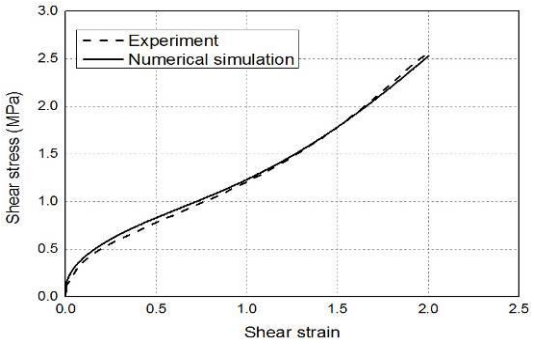

(b) Strain rate of 0.8 1/s

Figure 5.1 Comparison of numerical simulation and monotonic shear test results of NRB

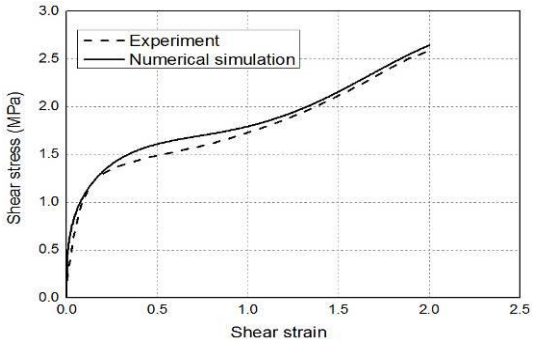

(a) Strain rate of 1.6 1/s

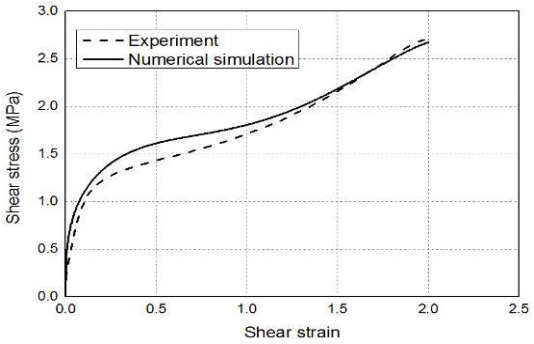

(b) Strain rate of 0.8 1/s

Figure 5.2 Comparison of numerical simulation and monotonic shear test results of HDRB

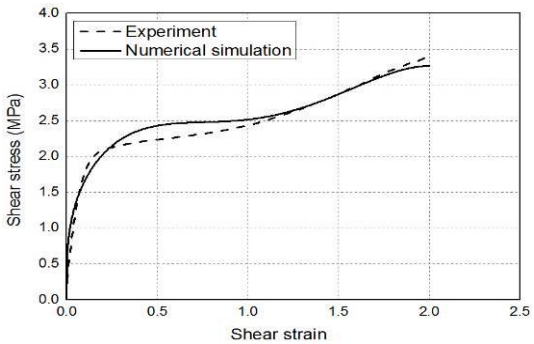

(a) Strain rate of 1.6 1/s

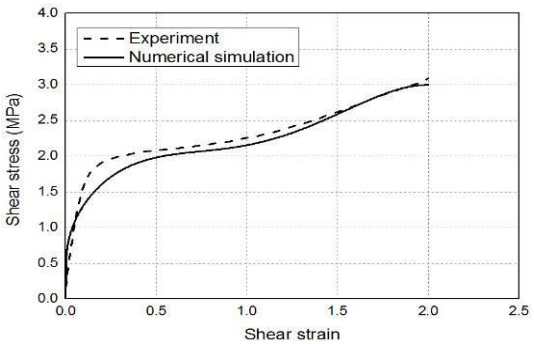

(b) Strain rate of 0.8 1/s

Figure 5.3 Comparison of numerical simulation and monotonic shear test results of SHDRB

6. CONCLUSIONS

This study proposed a general mathematical expression to accurately represent the rate-dependent

force-displacement relationship of three types of elastomeric bearings. Comparing the simulations using the model with test results, it is concluded that the proposed model can reproduce the behavior of elastomeric bearing accurately.

ACKNOWLEDGEMENTS

The authors gratefully acknowledge the financial support from National Science Foundation of China (No. 51278219).

REFERENCE

[1] Japan Road Association. (2002). Specifications for highway bridges. Part V: seismic design.

[2] Abe M, Yoshida J, Fujino Y. (2004). Multiaxial Behaviors of Laminated Rubber Bearings and Their Modeling. II: Modeling. *Journal of Structural Engineering*. **130:8**, 1133-1144.

[3] Bhuiyan A R, Okui Y, Mitamura H, et al. (2009). A rheology model of high damping rubber bearings for seismic analysis: Identification of nonlinear viscosity. *International Journal of Solids and Structures*. **46:7-8**, 1778-1792.

[4] Rivlin R S. (1948). Large elastic deformations of isotropic materials IV. Further developments of the general theory. *Philos Trans R Soc*. **A241**, 379–397.

[5] Amin, A.F.M.S., Wiraguna, S.I., Bhuiyan, A.R., Okui, Y. (2006). Hyperelasticity model for Finite Element analysis of natural and high damping rubbers in compression and shear. *J. Eng. Mech., ASCE*.**132:1**, 1–11.

[6] Huber N, Tsakmakis C. (2000). Finite deformation viscoelasticity laws. *Mechanics of Materials*. **32:1**, 1-18.